Trypanothione-dependent glyoxalase I in *Trypanosoma cruzi*

Neil GREIG, Susan WYLLIE, Tim J. VICKERS[1] and Alan H. FAIRLAMB[2]

Division of Biological Chemistry and Molecular Microbiology, Wellcome Trust Biocentre, College of Life Sciences, University of Dundee, Dundee, DD1 5EH, Scotland, U.K.

The glyoxalase system, comprizing glyoxalase I and glyoxalase II, is a ubiquitous pathway that detoxifies highly reactive aldehydes, such as methylglyoxal, using glutathione as a cofactor. Recent studies of *Leishmania major* glyoxalase I and *Trypanosoma brucei* glyoxalase II have revealed a unique dependence upon the trypanosomatid thiol trypanothione as a cofactor. This difference suggests that the trypanothione-dependent glyoxalase system may be an attractive target for rational drug design against the trypanosomatid parasites. Here we describe the cloning, expression and kinetic characterization of glyoxalase I from *Trypanosoma cruzi*. Like *L. major* glyoxalase I, recombinant *T. cruzi* glyoxalase I showed a preference for nickel as its metal cofactor. In contrast with the *L. major* enzyme, *T. cruzi* glyoxalase I was far less fastidious in its choice of metal cofactor efficiently utilizing cobalt, manganese and zinc. *T. cruzi* glyoxalase I isomerized hemithioacetal adducts of trypanothione more than 2400 times more efficiently than glutathione adducts, with the methylglyoxal adducts 2–3-fold better substrates than the equivalent phenylglyoxal adducts. However, glutathionylspermidine hemithioacetal adducts were most efficiently isomerized and the glutathionylspermidine-based inhibitor *S*-4-bromobenzylglutathionylspermidine was found to be a potent linear competitive inhibitor of the *T. cruzi* enzyme with a K_i of 5.4 ± 0.6 μM. Prediction algorithms, combined with subcellular fractionation, suggest that *T. cruzi* glyoxalase I localizes not only to the cytosol but also the mitochondria of *T. cruzi* epimastigotes. The contrasting substrate specificities of human and trypanosomatid glyoxalase enzymes, confirmed in the present study, suggest that the glyoxalase system may be an attractive target for anti-trypanosomal chemotherapy.

Key words: drug discovery, glyoxalase, methylglyoxal, trypanothione.

INTRODUCTION

Chagas' disease, or American trypanosomiasis, is caused by the flagellated protozoan parasite *Trypanosoma cruzi*. Despite a marked reduction in rates of transmission in countries such as Brazil, Chile and Uruguay over the last 20 years, the disease remains a major health risk in many Latin American countries with more than 15 million infected people and an annual death toll of approx. 13 000 [1]. The efficacy of the current nitro-drugs, nifurtimox and benznidazole, is poor, particularly in the chronic stage of infection. Both drugs have a high incidence of side effects [2] so that many patients are unable to complete a full course of treatment. Consequently, identification of novel drug targets and more effective replacement drug therapies has now become a matter of urgency.

In the search for antiparasitic drug targets, biochemical pathways that are both essential for parasite survival and absent from the host are sought after [3]. One such pathway is the thiol metabolism of trypanosomes and *Leishmania*. These parasites are uniquely dependent upon $T[SH]_2$ [trypanothione, N^1,N^8-bis(glutathionyl) spermidine] as their principal low-molecular-mass thiol, which, together with trypanothione reductase, assumes many of the antioxidant functions commonly undertaken by glutathione and glutathione reductase in their human hosts [4]. In related trypanosomatids, $T[SH]_2$ has already been implicated in the mode of action as well as the mechanism of resistance of antimonial drugs in *Leishmania* spp. [5–7] and in defence against chemical and oxidant stress induced by arsenicals and nifurtimox in African trypanosomes [8–10]. Therefore, in an attempt to exploit this essential and unique metabolic pathway, trypanothione-dependent enzymes have become a major focus for drug discovery against these neglected tropical diseases.

In our previous study [11], we reported the characterization of the $T[SH]_2$-dependent enzyme GLO1 (glyoxalase I) in *L. major*. This finding, combined with the identification of $T[SH]_2$-dependent GLO2 in both *Trypanosoma brucei* [12] and *L. donovani* [13], provides compelling evidence for a unique $T[SH]_2$-dependent glyoxalase system in certain trypanosomatids. The glyoxalase system is a ubiquitous pathway for the detoxification of highly reactive oxoaldehydes. The metalloenzymes glyoxalase I (lactoylglutathione lyase) and glyoxalase II (hydroxyacylglutathione lyase) catalyse the step-wise dismutation of 2-oxoaldehydes into the corresponding 2-hydroxyacids, using glutathione as a cofactor [14,15]. The principal role of the glyoxalase system is thought to be the detoxification of methylglyoxal (2-oxopropanal), a highly toxic α-oxoaldehyde produced as a by-product of glycolysis and possessing cytotoxic, cytostatic and mutagenic properties [16]. In addition, methylglyoxal is also produced by the catabolism of threonine via aminoacetone or hydroxyacetone [17]. The inherent toxicity of this molecule stems from its propensity to react with the nucleophilic centres of DNA, RNA and proteins. In particular, the oxoaldehyde reacts with the side chains of arginine, lysine and cysteine, and with the base guanine.

Inhibitors of GLO1 exhibit anticancer and antimalarial properties and are selectively toxic for rapidly proliferating cells [18]. The $T[SH]_2$-dependent glyoxalase system may provide an ideal target for Chagas' disease drug development. With this in mind, here we describe the expression, purification and kinetic characterization of GLO1 from *T. cruzi*.

Abbreviations used: ECL, enhanced chemiluminesence; GLO1, glyoxalase I; *Tc*GLO1, *Trypanosoma cruzi* GLO1; MALDI–TOF-MS, matrix-assisted laser-desorption ionization–time-of-flight MS; TCEP, tris(2-carboxyethyl)phosphine; $T[SH]_2$, trypanothione, N^1,N^8-bis(glutathionyl)spermidine.

[1] Current address: Department of Molecular Microbiology, Washington University School of Medicine, St. Louis, MO 63110-1093, U.S.A.

[2] To whom correspondence should be addressed (email a.h.fairlamb@dundee.ac.uk).

© 2006 Biochemical Society

EXPERIMENTAL

Materials

Methylglyoxal was prepared from methylglyoxal dimethylacetal and confirmed to be free of formaldehyde, as described previously [19]. All other reagents were standard commercial products of high purity.

Cloning and expression of *Tc*GLO1 (*T. cruzi* GLO1)

A putative *T. cruzi GLO1* gene (Tc00.1047053510659.240) was identified in the *T. cruzi* genome database (www.genedb.org). This gene was amplified by PCR from *T. cruzi* CL Brener genomic DNA using the sense primer: 5′ CATATGTCAACACGACGACTTATGCACACGATG 3′ with an additional NdeI site (underlined); and the antisense primer: 5′ GGATCCGGATCCTTAAGCCGTTCCCTGTTC 3′ with an additional BamHI site (underlined). The PCR product was then cloned into the pCR®-Blunt II-TOPO® vector (Invitrogen) and sequenced. The pCR®-Blunt II-TOPO®-*Tc*GLO1 constructs were then digested with NdeI and BamHI and the fragments cloned into the pET15b expression vector (Novagen) resulting in a pET15b-*Tc*GLO1 construct.

Transformed BL21(DE3)pLysS *Escherichia coli* cells were grown in Luria–Bertani medium containing 100 μg/ml ampicillin and 12.5 μg/ml chloramphenicol to a D_{600} of $\sim$0.6. Expression was induced with 1 mM isopropyl-β-D-thiogalactoside for 4 h at 25 °C. Following expression, cells were pelleted (3000 ***g*** for 10 min at 4 °C), resuspended in lysis buffer [75 mM sodium phosphate, pH 7.5, 500 mM NaCl, 10 mM 2-mercaptoethanol and protease inhibitor cocktail (Roche)] and then lysed by sonication (four 30 s bursts at 15 microns amplitude), with cooling between pulses. The lysate was centrifuged (30 000 ***g*** for 30 min) and the supernatant loaded at 2 ml/min onto a 5 ml HiTrap™ chelating Sepharose column (Amersham Pharmacia) in 50 mM sodium phosphate (pH 7.5) and 200 mM NaCl. *Tc*GLO1 was eluted with a gradient of 0 to 500 mM imidazole in the same buffer. Eluted protein was then dialysed against 25 mM Bis-Tris, pH 6.5 and loaded onto a 5 ml HiTrap™ Q-Sepharose column (Amersham Pharmacia) at 2 ml/min and eluted with a gradient of 0–500 mM NaCl in the same buffer. Finally, the N-terminal His_6-tag was removed by thrombin cleavage (30 units/mg for 12 h at 25 °C) and untagged *Tc*GLO1 was recovered using a HiTrap™ Q-Sepharose column, as described previously [11].

Physical properties of *Tc*GLO1

The native M_r of *Tc*GLO1 was determined using Superdex 200 HR 10/30 size exclusion column chromatography (Amersham Pharmacia) against gel filtration standards (Bio-Rad). Molecular mass was determined by MALDI–TOF-MS (matrix-assisted laser-desorption ionization–time-of-flight MS) in linear mode using sinapinic acid as a matrix on a Voyager-DE STR mass spectrometer (PerSeptive Biosystems).

Production of thiols

Trypanothione disulfide (Bachem) was reduced using TCEP [tris(2-carboxyethyl)phosphine] agarose, as described previously [11].

Apoenzyme production and metal reconstitution

Apoenzyme was prepared by dialysis of *Tc*GLO1 for 24 h [11] against 1 litre of 20 mM imidazole, 1 mM EDTA, pH 7.0 containing 5 g Chelex resin (2 volume changes). The enzyme was then reconstituted by incubation with a 10-fold molar excess of metal chloride in Chelex-treated 50 mM Hepes, pH 7.0, for 10 min at room temperature (25 °C).

Kinetic analysis of *Tc*GLO1 activity

The pH optimum for the enzyme was determined over the pH range 4–10 using a mixed buffer system of 50 mM each of Ches [2-(*N*-cyclohexylamino)ethanesulfonic acid], Hepps and Mes (pH adjusted using KOH). The effect of ionic strength on enzyme activity was determined as above in 50 mM Hepes (pH 7.0) with various concentrations (0.025–0.4 M) of NaCl and $(NH_4)_2SO_4$. To ensure that $NiCl_2$ co-factor was not a limiting factor for enzyme activity in these assays, *Tc*GLO1 was pre-incubated with a 10-fold molar excess of $NiCl_2$.

Kinetic constants (K_m and k_{cat}) and pH optimization studies were determined by measuring the rate of isomerized hemithioacetal adduct formation at 240 nm using a continuous spectrophotometric assay (Shimadzu UV-2401 PC dual beam Spectrophotometer) [11]. The rate of phenylglyoxal adduct formation was measured at 263 nm. Hemithioacetal concentrations were calculated using the previously established K_d values of 3.0 mM for the methylglyoxal-thiol adduct and 0.6 mM for the phenylglyoxal-thiol adduct [20], in the presence of 0.1 M reduced thiol. Assays (0.5 ml) were performed in 50 mM Hepes/KOH (pH 7.0) with 25 mM NaCl at 27 °C. With the methylglyoxal and phenylglyoxal glutathione hemithioacetals, k_{cat}/K_m values were determined from the slope of rates plotted against enzyme concentration.

Inhibitor studies

Inhibition constants for *Tc*GLO1 were determined over a range of substrate concentrations (0.5–2.5 times the K_m with the hemithioacetal of trypanothione) at three fixed concentrations of *S*-4-bromobenzylglutathionylspermidine [21]. Linear Lineweaver–Burk transformations of each data set were inspected for the inhibition pattern and found to be competitive. Data sets were fitted by non-linear regression using the GraFit program and kinetic parameters determined.

Western analyses of cell extracts

Polyclonal antiserum against *L. major* GLO1 was raised in adult male Wistar rats. An initial injection of 100 μg of purified antigen [11], emulsified in complete Freund's adjuvant, was followed by two identical booster injections of antigen emulsified in Freund's incomplete adjuvant at 2-week intervals. *L. major* promastigotes (Friedlin strain; World Health Organization designation: MHOM/JL/81/Friedlin; 2×10^7 ml^{-1}, 1 litre) and *T. cruzi* epimastigotes (CL Brener, genome project standard clone; 3×10^7 ml^{-1}, 1 litre) were pelleted by centrifugation (1600 ***g*** for 10 min at 4 °C), washed twice in 20 mM Tris/HCl (pH 7.0) containing 0.1 mM sucrose and re-suspended in cell lysis buffer (10 mM Hepes, pH 7.0). For biological safety, parasites were inactivated by three cycles of freezing in liquid nitrogen and thawing in a 37 °C water bath, before lysis under pressure (30 klbf/in^2; 1 lb/in^2 $\equiv$ 6.9 kPa) using a one shot cell disruptor (Constant Systems). Following centrifugation (20 000 ***g*** for 40 min), cell supernatant was collected and protein concentration determined. Whole cell extracts (30 μg) were then separated by SDS/PAGE (12 % gels) and subsequently transferred onto nitrocellulose. After blocking with 5 % (w/v) skimmed milk in PBS at room temperature for 1 h, the blot was incubated with *L. major* GLO1 polyclonal antiserum (1:700 dilution) at room temperature for 1 h, washed in PBS containing 0.1 % (v/v) Tween 20 and

© 2006 Biochemical Society

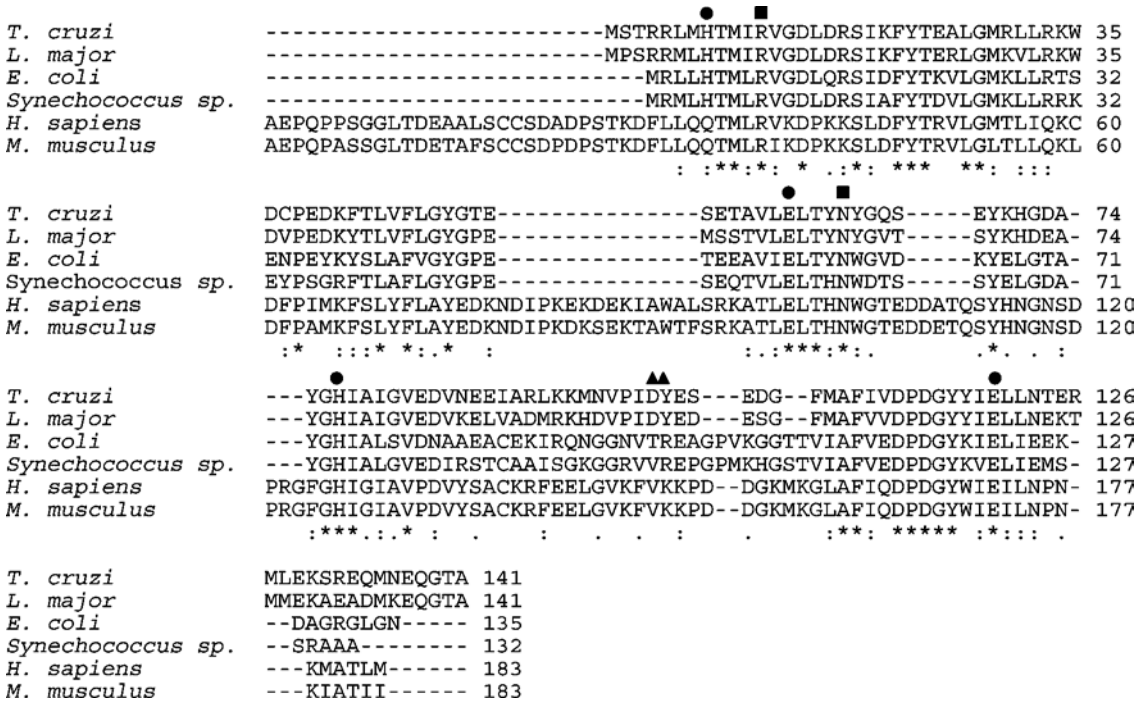

Figure 1 Alignment of the predicted amino acid sequences of glyoxalase I

Gaps introduced into sequences to optimize alignments are represented by dashes. Conserved and similar residues are indicated by asterisks and dots respectively. The circles indicate conserved metal binding residues in the various sequences. Squares indicate conserved residues implicated in the binding of γ-glutamate moieties of thiol cofactors while triangles highlight conserved acidic residues (Asp^{100} and Tyr^{101}) in the trypanosomatid enzymes thought to be involved in the binding of $T[SH]_2$ [28]. Protein sequences are from *T. cruzi* (Tc00.1047053510659), *L. major* (LmjF35.3010), *E. coli* (Swiss-Prot accession no. P77036), *Synechoccus* sp. WH 8102 (TrEMBL accession no. Q7U3T2), human (Swiss-Prot accession no. P78375) and mouse (Swiss-Prot accession no. Q9CPU0).

then incubated with a secondary rabbit anti-rat (IgG) antibody (1:10000 dilution; Dako). The immunoblot was subsequently developed using the ECL® (enhanced chemiluminescence) Plus system from Amersham Biosciences.

Subcellular fractionation

Subcellular fractions of *L. major* promastigotes and *T. cruzi* epimastigotes were prepared essentially as described previously [22]. Each fraction (30 μg) was then separated by SDS/PAGE (12 % gels) and transferred onto nitrocellulose. After blocking, the blot was probed with *L. major* GLO1 polyclonal antiserum and detected by chemiluminescence, as described above. Following analysis, the immunoblot was stripped using Restore Western Blot Stripping Buffer (Pierce) and reprobed using the following primary antibodies in turn: anti-Hsp60 monoclonal antibody (1:5000 dilution; Stressgen); anti-(*L. major* trypanothione synthetase) antiserum (1:1000 dilution; [22]) and anti-(*T. brucei* BiP) antiserum (1:5000; [23]). Rabbit anti-rat (IgG) antibody (1:10000 dilution) and anti-(mouse IgG–horseradish peroxidase) antibody (1:10000 dilution; Sigma) were used as secondary antibodies where appropriate, and immunoblots were once again developed by ECL®.

RESULTS AND DISCUSSION

Identification of *T. cruzi* GLO1 sequences

The identification of a unique trypanothione-dependent glyoxalase system within *Leishmania* spp. and *T. brucei* [11–13] has raised hopes that the enzymes of this pathway may provide suitable targets for rational drug design against all trypanosomatids. However, despite having certain unique metabolic features in common [24], the evolutionary distance between *Leishmania* and *Trypanosoma* is large, approaching that of the fly and human [25]. With this in mind, we have determined the physicochemical and kinetic properties of GLO1 from *T. cruzi*.

BLAST searches of the *T. cruzi* genome database, using *E. coli* and *L. major* GLO1 sequences as templates, revealed a 426 bp sequence (Tc00.1047053510659.240) which shared 72 % and 44 % sequence identity to the *L. major* and *E. coli* GLO1 sequences respectively. Alignment of the putative *Tc*GLO1 along with other trypanosomatid, eukaryotic and bacterial GLO1 amino acid sequences (Figure 1) illustrated a high degree of similarity between the trypanosomatid and bacterial GLO1 proteins. Similarity with the eukaryotic GLO1 sequences was between 39.4 and 32.4 %, with mammalian enzymes differing in that they have a number of unique insertions and an N-terminal extension. The conservation of a histidine residue near the N-terminus of the trypanosomatid proteins (residue 8 in *T. cruzi*) is suggestive of a nickel cofactor-binding site. However, in eukaryotic sequences a conserved glutamine in the same position is indicative of a zinc cofactor-binding site [26]. Conserved acidic residues (Asp^{100} and Tyr^{101}) in the trypanosomatid enzymes are believed to be involved in the specific binding of $T[SH]_2$ [21].

Cloning and expression of *Tc*GLO1 in *E. coli*

Sequence-specific sense and anti-sense primers were used to amplify the 426 bp *TcGLO1* gene from *T. cruzi* CL Brener genomic DNA by PCR. The product was sub-cloned into the pCR®-Blunt II-TOPO® vector, sequenced to verify identity and cloned into pET15b giving the plasmid pET15b-*Tc*GLO1. The resulting plasmid contains the entire open reading frame of *Tc*GLO1 fused in frame with a cleavable His_6-tag at the N-terminus.

© 2006 Biochemical Society

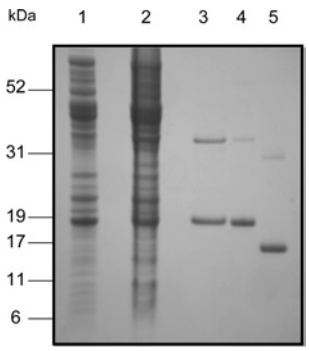

Figure 2 Purification of recombinant *Tc*GLO1

Lane 1, soluble fraction of BL21 (DE3)pLysS [pET15b-*Tc*GLO1], uninduced cells; lane 2, soluble fraction of BL21 (DE3)pLysS [pET15b-*Tc*GLO1], induced cells; lane 3, pooled fractions from nickel affinity chromatography; lane 4, pooled fractions from anion exchange chromatography (Resource-Q); lane 5, pooled fractions from anion exchange chromatography (Resource-Q) after removal of the His_6-tag with thrombin protease.

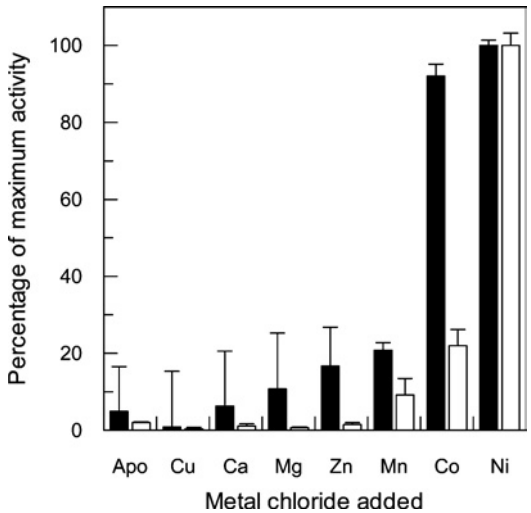

Figure 3 Metal reconstitution of *Tc*GLO1 in various bivalent metal chlorides

The apo form of *Tc*GLO1 was incubated with a 10-fold molar excess of bivalent metal ions for 10 min at room temperature. Assays contained 25 μM trypanothione hemithioacetal and 0.1 mM free $T[SH]_2$. *L. major* GLO1 reconstituted activity (black bars; [11]) is shown next to the *Tc*GLO1 data (white bars). All assays were performed in triplicate, with the mean activity relative to the nickel-activated enzymes displayed.

E. coli BL21(DE3)pLysS transformed with pET15b-*Tc*GLO1 produced soluble and enzymatically active protein. *Tc*GLO1 was purified to homogeneity via nickel affinity and anion exchange chromatography. The N-terminal His_6-tag was then removed by thrombin cleavage followed by a second anion exchange chromatography step (Figure 2). No residual His_6-tagged enzyme could be detected by SDS/PAGE and Western analysis with an anti-His_6 antibody. Both His_6-tagged and untagged *Tc*GLO1 readily formed dimers that were resistant to SDS denaturation and reduction with dithiotheitol, TCEP or 2-mercaptoethanol. Typical yields were between 5 and 7 mg/litre of starting culture.

Determination of *Tc*GLO1 physical properties

SDS/PAGE analysis of *Tc*GLO1 revealed a recombinant protein with an apparent molecular mass of 17 kDa (18.5 kDa with the His_6-tag), in good agreement with the predicted size (16647 Da). The nominal molecular mass of recombinant *Tc*GLO1 was determined to be 16650 Da by MALDI–TOF-MS analysis. Size exclusion chromatography and analytical ultracentrifugation showed native *Tc*GLO1 to actively form dimers in solution with an M_r of 31300 (results not shown). These physiological properties are in good agreement with those for *L. major* GLO1 [11].

Metal specificity of *Tc*GLO1

Sequence analyses suggested that nickel was likely to be the preferred metal cofactor of *Tc*GLO1. To test this assumption, a range of bivalent cations were analysed for their ability to reactivate enzyme activity in the *Tc*GLO1 apo-protein (Figure 3). Like the *Leishmania* enzyme, nickel was found to be the most effective in reactivating glyoxalase I enzyme activity. However, reactivation by cobalt was found to be only marginally less effective than nickel. Indeed, in comparison with the *L. major* enzyme, *Tc*GLO1 was found to be far less fastidious in its choice of metal cofactor, with both zinc and manganese capable of significant levels of reactivation. The versatility of *Tc*GLO1 in utilizing a wider range of metal cofactors might be due to differing bioavailability in the mammalian host cells parasitized or in their respective insect vectors.

Kinetic characterization

Using a mixed buffer system, the optimum for *Tc*GLO1 activity was determined to be pH 7.0 (Figure 4A). Interestingly, a rapid decline in enzyme activity was noted in mildly alkaline conditions. This loss in *Tc*GLO1 activity was subsequently shown to be reversible indicating that it is not due to denaturation at alkaline pH (results not shown). In 50 mM Hepes buffer at the optimum pH the optimum ionic conditions of the assay were found to be 25 mM NaCl (Figure 4B). *L. major* GLO1 has a high degree of substrate specificity for trypanothione hemithioacetals in preference to glutathione hemithioacetals [11], the substrate of choice for human GLO1 [16]. Similarly, *Tc*GLO1 isomerized hemithioacetal adducts of trypanothione and glutathionylspermidine 2400 and 14000 times more efficiently than glutathione adducts respectively (Table 1). Of these two preferred substrates, *Tc*GLO1 had a significantly higher affinity for the glutathionylspermidine adducts with either methylglyoxal or phenylglyoxal, as demonstrated by a markedly lower K_m value, resulting in a 6-fold difference in k_{cat}/K_m. The *T. cruzi* enzyme displayed substrate specificity based not only upon thiol cofactor, but also on the oxoaldehyde component of the hemithioacetal. Methylglyoxal adducts were found to be between 2- and 3-fold better substrates than the equivalent phenylglyoxal adducts. The most striking difference between the *L. major* and *T. cruzi* enzymes is the 5-fold greater efficiency with which the *L. major* enzyme utilizes trypanothione hemithioacetals. This observation may be explained by the significantly lower intracellular levels of trypanothione in *L. major* promastigotes [27].

While glutathionylspermidine adducts appear to be the most efficient substrate for *Tc*GLO1, 6-fold more efficient that trypanothione hemithioacetals, it should be noted that trypanothione levels are 8-fold higher than gluthionylspermidine in *T. cruzi* epimastigotes [27]. Based on their relevant ratios it would seem that both glutathionylspermidine and trypanothione hemithioacetal adducts may act as the physiological substrates of the *T. cruzi* enzyme *in vivo*. The mutually exclusive substrate specificities of the human and parasitic GLO1 enzymes have been directly related to major differences in active site architecture [28]. It is hoped that these differences can be exploited in the structure-based design of selective inhibitors against the trypanosomatids.

© 2006 Biochemical Society

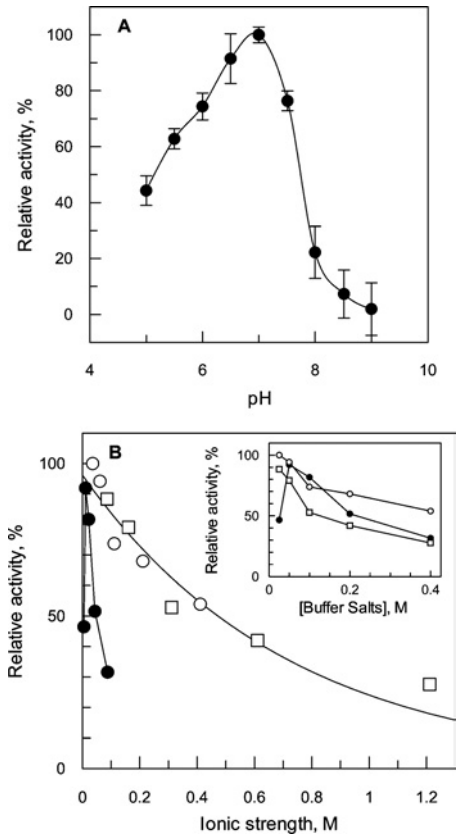

Figure 4 Enzymatic characterization of *Tc*GLO1

(**A**) Determination of assay pH optimum. Assays were performed with 50 μM trypanothione hemithioacetal in a mixed buffer system, as described in the Materials and methods section. Activity is expressed as a percentage relative to the maximum activity determined for *Tc*GLO1. Results are presented as means $\pm$ S.D. from three measurements. (**B**) Effect of buffer concentration and ionic strength on *Tc*GLO1 activity. The assay mixtures contained either various amounts of Hepes buffer, pH 7.0 (closed circles), NaCl (open circles), or $(NH_4)_2SO_4$ (open squares). Activity is expressed as a percentage of the activity determined in 50 mM Hepes buffer/25 mM NaCl. The inset shows the effect on activity as a function of buffer or salt concentration.

Table 1 Kinetic properties of *T. cruzi* GLO1

Kinetic constants (K_m and k_{cat}) were determined as described previously [11]. Results are means $\pm$ S.D. for triplicate measurements. ND, not determined.

Hemithioacetal substrate	K_m, μM	k_{cat}, s^{-1}	$k_{cat}/K_m \times 10^6 \cdot M^{-1} \cdot s^{-1}$	k_{cat}/K_m (relative)
Glutathionylspermidine				
Methylglyoxal	8.0 $\pm$ 0.4	161 $\pm$ 12	20	100
Phenylglyoxal	14 $\pm$ 2.1	105 $\pm$ 28	7.5	37.5
Trypanothione				
Methylglyoxal	109 $\pm$ 10	363 $\pm$ 33	3.3	16.5
Phenylglyoxal	207 $\pm$ 23	265 $\pm$ 31	1.5	7.5
Glutathione				
Methylglyoxal	>1800	ND	0.0014	0.007
Phenylglyoxal	>1800	ND	0.0005	0.0025

Inhibitor studies

The high affinity of the trypanosomatid GLO1 enzymes for glutathionylspermidine adducts may be useful in the future design of substrate-mimetic competitive inhibitors. (*S*)-4-Bromobenzylglutathionylspermidine was found to be a linear competitive inhibitor of GLO1 with respect to trypanothione hemithioacetal,

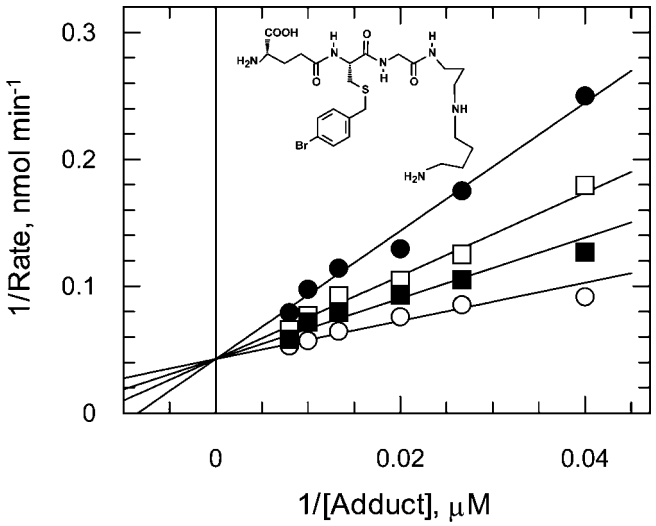

Figure 5 *S*-4-bromobenzylglutathionylspermidine inhibition of *Tc*GLO1

*Tc*GLO1 inhibition constants were determined at three fixed concentrations of the inhibitor [(*S*)-4-bromobenzylglutathionylspermidine] and over a range of substrate concentrations (25–125 μM trypanothione hemithioacetal). Data sets for each inhibitor concentration were fitted by non-linear regression and are presented as Lineweaver–Burk transformations. Trypanothione hemithioacetal was varied in the presence of 0 (○), 3.15 (■), 6.3 (□) and 12.6 μM (●) (*S*)-4-bromobenzylglutathionylspermidine.

as shown by diagnostic Lineweaver–Burk plots (K_i of 5.4 $\pm$ 0.6 μM, Figure 5) which is 10-fold higher than for the *L. major* enzyme [28]. Comparison of *L. major* GLO1 with a homology model of *Tc*GLO1 did not identify any striking differences between the active sites of both enzymes that could account for differences in inhibitor potency (T. Ariza and C. Bond, unpublished results). In contrast with the glutathionylspermidine analogue, *S*-4-bromobenzylglutathione is inactive as an inhibitor of both trypanosomatid enzymes (results not shown).

Substrate analogues have been successfully used as inhibitors against GLO1 in several other organisms [29–31]. For example, (*S*)-(*N*-aryl-*N*-hydroxycarbamoyl)glutathione and (*S*)-(*N*-alkyl-*N*-hydroxycarbamoyl)glutathione compounds have been shown to inhibit human GLO1 with K_i values in the nanomolar range [32] and in the form of a diester to rapidly kill proliferating cancer cells [33]. It is tempting to suggest that the glutathionylspermidine version of these compounds may selectively inhibit trypanosomatid GLO1 activity and in their diester forms may prove to be toxic for parasites.

Western analyses of cell extracts and subcellular fractions

Immunoblots of *L. major* promastigote and *T. cruzi* epimastigote whole cell lysates were probed with a *L. major* GLO1-specific polyclonal antiserum (Figure 6A). As expected, a 17 kDa protein equivalent to the predicted molecular mass of the GLO1 enzymes reacted strongly with the antiserum in both the *L. major* and the *T. cruzi* lysates. Crude subcellular fractions of *L. major* promastigotes were also prepared and analysed by Western blot (Figure 6B). The purity of each fraction was demonstrated using antibodies against marker proteins in each subcellular location. The endoplasmic reticulum-localized BiP protein was used as a marker for the microsomal fraction while Hsp60 and trypanothione synthetase were used as marker proteins for the large granular and cytosolic fractions respectively. Interestingly, GLO1 was found to localize not only in the cytosol, but also in the large granular fraction from these parasites. Similar GLO1 localization

© 2006 Biochemical Society

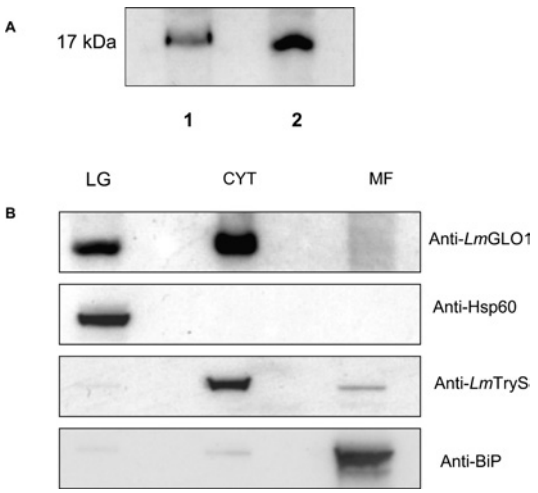

Figure 6 Immunoblot analysis of cell lysates and cellular localization of *Tc*GLO1

(**A**) Blots of whole cell extracts (30 μg of protein in each lane) from *T. cruzi* epimastigotes (lane 1) and *L. major* promastigotes (lane 2) were probed with an anti-(*L. major* GLO1) antiserum. (**B**) Subcellular fractions of *L. major* promastigotes, containing the large granule (LG), cytosol (C), and microsomal fractions (MF), were prepared as described in the Materials and methods section. Western blots of these equally loaded fractions (30 μg of protein in each lane) were probed with anti-(*L. major* GLO1) antibody. In addition, blots were stripped and reprobed with antiserum to marker proteins for each subcellular fraction to demonstrate the purity of each fraction [LG, anti-Hsp60; C, anti-(*L. major* trypanothione synthetase); and MF, anti-BiP].

was observed in lysates of *T. cruzi* epimastigotes (results not shown). Subsequent analysis of the *Tc*GLO1 and *L. major* GLO1 primary sequences with MitoProt II [34], used to predict targeting of proteins to the mitochondria, suggested that both enzymes are likely to be exported to the mitochondria with a $P = 0.909$ and 0.8704 respectively. However, no cleavage site was predicted for the mitochondrial targeting sequences of either protein.

While comparatively little is known about the cellular location of GLO1 enzymes in other organisms, GLO2 has been extensively studied and detected in the cytoplasm and mitochondria of several higher eukaryotes including rat [35], human [36], yeast [37] and *Arabidopsis thaliana* [38]. In higher plants and yeast, distinct genes encode the alternate forms of GLO2, whereas analysis of GLO2 mRNA sequences in vertebrates indicates that dual initiation from alternative AUG codons is responsible [36]. In our future studies we hope to explore the targeting mechanism of GLO1 to trypanosomatid mitochondria.

In conclusion, the contrasting substrate specificities of human and trypanosomatid glyoxalase enzymes suggest that the glyoxalase system may be an attractive target for anti-trypanosomal chemotherapy. Gene knockout studies are underway to determine the role this pathway plays in parasite growth, survival or virulence.

We would like to thank Ian Eggleston and colleagues for providing inhibitors for this and previous studies, Charlie Bond and Tony Ariza for modelling studies, Irene Hallyburton for AUC and Douglas Lamont for performing mass spectrometry (all from the Division of Biological Chemistry and Molecular Microbiology, Wellcome Trust Biocentre, College of Life Sciences, University of Dundee, Dundee, DD1 5EH, Scotland, U.K.). This work was funded by the Wellcome Trust.

REFERENCES

1 World Health Organization (2002) The World health report 2002: reducing risks, promoting healthy life, World Health Organization, Geneva
2 Castro, J. A. and Diaz-de-Toranzo, E. G. (1988) Toxic effects of nifurtimox and benznidazole, two drugs used against American trypanosomiasis (Chagas' disease). Biomed. Environ. Sci. **1**, 19–33
3 El Sayed, N. M., Myler, P. J., Blandin, G., Berriman, M., Crabtree, J., Aggarwal, G., Caler, E., Renauld, H., Worthey, E. A., Hertz-Fowler, C. et al. (2005) Comparative genomics of trypanosomatid parasitic protozoa. Science **309**, 404–409
4 Fairlamb, A. H. and Cerami, A. (1992) Metabolism and functions of trypanothione in the Kinetoplastida. Annu. Rev. Microbiol. **46**, 695–729
5 Wyllie, S., Cunningham, M. L. and Fairlamb, A. H. (2004) Dual action of antimonial drugs on thiol redox metabolism in the human pathogen *Leishmania donovani*. J. Biol. Chem. **279**, 39925–39932
6 Croft, S. L., Sundar, S. and Fairlamb, A. H. (2006) Drug resistance in Leishmaniasis. Clin. Microbiol. Rev. **19**, 111–126
7 Mukhopadhyay, R., Dey, S., Xu, N., Gage, D., Lightbody, J., Ouellette, M. and Rosen, B. P. (1996) Trypanothione overproduction and resistance to antimonials and arsenicals in *Leishmania*. Proc. Natl. Acad. Sci. U.S.A. **93**, 10383–10387
8 Alibu, V. P., Richter, C., Voncken, F., Marti, G., Shahi, S., Renggli, C. K., Seebeck, T., Brun, R. and Clayton, C. (2006) The role of *Trypanosoma brucei* MRPA in melarsoprol susceptibility. Mol. Biochem. Parasitol. **146**, 38–44
9 Fairlamb, A. H., Henderson, G. B. and Cerami, A. (1989) Trypanothione is the primary target for arsenical drugs against African trypanosomes. Proc. Natl. Acad. Sci. U.S.A. **86**, 2607–2611
10 Ariyanayagam, M. R., Oza, S. L., Guther, M. L. and Fairlamb, A. H. (2005) Phenotypic analysis of trypanothione synthetase knockdown in the African trypanosome. Biochem. J. **391**, 425–432
11 Vickers, T. J., Greig, N. and Fairlamb, A. H. (2004) A trypanothione-dependent glyoxalase I with a prokaryotic ancestry in *Leishmania major*. Proc. Natl. Acad. Sci. U.S.A. **101**, 13186–13191
12 Irsch, T. and Krauth-Siegel, R. L. (2004) Glyoxalase II of African trypanosomes is trypanothione-dependent. J. Biol. Chem. **279**, 22209–22217
13 Padmanabhan, P. K., Mukherjee, A. and Rentala, M. (2005) Characterization of the gene encoding glyoxalase II from *Leishmania donovani*: a potential target for anti-parasite drug. Biochem. J. **393**, 227–234
14 Thornalley, P. J. (1990) The glyoxalase system: new developments towards functional characterization of a metabolic pathway fundamental to biological life. Biochem. J. **269**, 1–11
15 Vander Jagt, D. L., Hunsaker, L. A., Kibirige, M. and Campos, N. M. (1989) NADPH production by the malarial parasite *Plasmodium falciparum*. Blood **74**, 471–474
16 Thornalley, P. J. (1996) Pharmacology of methylglyoxal: formation, modification of proteins and nucleic acids, and enzymatic detoxification – a role in pathogenesis and antiproliferative chemotherapy. Gen. Pharmacol. **27**, 565–573
17 Phillips, S. A. and Thornalley, P. J. (1993) The formation of methylglyoxal from triose phosphates. Investigation using a specific assay for methylglyoxal. Eur. J. Biochem. **212**, 101–105
18 Creighton, D. J., Zheng, Z. B., Holewinski, R., Hamilton, D. S. and Eiseman, J. L. (2003) Glyoxalase I inhibitors in cancer chemotherapy. Biochem. Soc. Trans. **31**, 1378–1382
19 Vince, R., Daluge, S. and Wadd, W. B. (1971) Studies on the inhibition of glyoxalase I by *S*-substituted glutathiones. J. Med. Chem. **14**, 402–404
20 Vander Jagt, D. L., Han, L. P. and Lehman, C. H. (1972) Kinetic evaluation of substrate specificity in the glyoxalase-I-catalysed disproportionation of ketoaldehydes. Biochemistry **11**, 3735–3740
21 Ariza, A., Vickers, T. J., Greig, N., Fairlamb, A. H. and Bond, C. S. (2005) Crystallization and preliminary X-ray analysis of *Leishmania major* glyoxalase I. Acta Crystallogr. Sect. F Struct. Biol. Cryst. Commun. **61**, 769–772
22 Oza, S. L., Shaw, M. P., Wyllie, S. and Fairlamb, A. H. (2005) Trypanothione biosynthesis in *Leishmania major*. Mol. Biochem. Parasitol. **139**, 107–116
23 Bangs, J. D., Uyetake, L., Brickman, M. J., Balber, A. E. and Boothroyd, J. C. (1993) Molecular cloning and cellular localization of a BiP homologue in *Trypanosoma brucei*. Divergent ER retention signals in a lower eukaryote. J. Cell Sci. **105**, 1101–1113
24 Berriman, M., Ghedin, E., Hertz-Fowler, C., Blandin, G., Renauld, H., Bartholomeu, D. C., Lennard, N. J., Caler, E., Hamlin, N. E., Haas, B. et al. (2005) The genome of the African trypanosome *Trypanosoma brucei*. Science **309**, 416–422
25 Fernandes, A. P., Nelson, K. and Beverley, S. M. (1993) Evolution of nuclear ribosomal RNAs in kinetoplastid protozoa: perspectives on the age and origins of parasitism. Proc. Natl. Acad. Sci. U.S.A. **90**, 11608–11612
26 Sukdeo, N., Clugston, S. L., Daub, E. and Honek, J. F. (2004) Distinct classes of glyoxalase I: metal specificity of the *Yersinia pestis*, *Pseudomonas aeruginosa* and *Neisseria meningitidis* enzymes. Biochem. J. **384**, 111–117
27 Ariyanayagam, M. R. and Fairlamb, A. H. (2001) Ovothiol and trypanothione as antioxidants in trypanosomatids. Mol. Biochem. Parasitol. **115**, 189–198

© 2006 Biochemical Society

28 Ariza, A., Vickers, T. J., Greig, N., Armour, K. A., Dixon, M. J., Eggleston, I. M., Fairlamb, A. H. and Bond, C. S. (2006) Specificity of the trypanothione-dependent *Leishmania major* glyoxalase I: structure and biochemical comparison with the human enzyme. Mol. Microbiol. **59**, 1239–1248
29 Kavarana, M. J., Kovaleva, E. G., Creighton, D. J., Wollman, M. B. and Eiseman, J. L. (1999) Mechanism-based competitive inhibitors of glyoxalase I: intracellular delivery, *in vitro* antitumor activities, and stabilities in human serum and mouse serum. J. Med. Chem. **42**, 221–228
30 Elia, A. C., Chyan, M. K., Principato, G. B., Giovannini, E., Rosi, G. and Norton, S. J. (1995) *N*,*S*-bis-fluorenylmethoxycarbonylglutathione – a new, very potent inhibitor of mammalian glyoxalase-II. Biochem. Mol. Biol. Int. **35**, 763–771
31 Thornalley, P. J., Strath, M. and Wilson, R. J. M. (1994) Antimalarial activity *in vitro* of the glyoxalase I inhibitor diester, *S*-p-bromobenzylglutathione diethyl ester. Biochem. Pharmacol. **47**, 418–420
32 Kalsi, A., Kavarana, M. J., Lu, T. F., Whalen, D. L., Hamilton, D. S. and Creighton, D. J. (2000) Role of hydrophobic interactions in binding S-*(N*-aryl/alkyl-*N*-hydroxycarbamoyl)glutathiones to the active site of the antitumor target enzyme glyoxalase I. J. Med. Chem. **43**, 3981–3986
33 Sharkey, E. M., O'Neill, H. B., Kavarana, M. J., Wang, H. B., Creighton, D. J., Sentz, D. L. and Eiseman, J. L. (2000) Pharmacokinetics and antitumor properties in tumor-bearing mice of an enediol analogue inhibitor of glyoxalase I. Cancer Chemoth. Pharm. **46**, 156–166
34 Claros, M. G. and Vincens, P. (1996) Computational method to predict mitochondrially imported proteins and their targeting sequences. Eur. J. Biochem. **241**, 779–786
35 Talesa, V., Uotila, L., Koivusalo, M., Principato, G., Giovannini, E. and Rosi, G. (1988) Demonstration of glyoxalase-II in rat-liver mitochondria: partial-purification and occurrence in multiple forms. Biochim. Biophys. Acta **955**, 103–110
36 Cordell, P. A., Futers, T. S., Grant, P. J. and Pease, R. J. (2004) The human hydroxyacylglutathione hydrolase (HAGH) gene encodes both cytosolic and mitochondrial forms of glyoxalase II. J. Biol. Chem. **279**, 28653–28661
37 Bito, A., Haider, M., Hadler, I. and Breitenbach, M. (1997) Identification and phenotypic analysis of two glyoxalase II encoding genes from *Saccharomyces cerevisiae*, GLO2 and GLO4, and intracellular localization of the corresponding proteins. J. Biol. Chem. **272**, 21509–21519
38 Maiti, M. K., Krishnasamy, S., Owen, H. A. and Makaroff, C. A. (1997) Molecular characterization of glyoxalase II from *Arabidopsis thaliana*. Plant Mol. Biol. **35**, 471–481

Received 13 June 2006/4 September 2006; accepted 8 September 2006
Published as BJ Immediate Publication 8 September 2006, doi:10.1042/BJ20060882

© 2006 Biochemical Society